Journal of Infection 92 (2026) 106760

Contents lists available at ScienceDirect

Journal of Infection

journal homepage: www.elsevier.com/locate/jinf

Viruses and Viral Diseases

Lymph node remodelling underlies the attenuated form of HIV/AIDS in people with HIV-2

Susana M. Fernandes [a,b,c], Guilherme B. Farias [a,b], Ana R. Pires [a,b], Diana F. Santos [a,b], Ana Vieira Antão [a,b], André Pires [a,b], Rita Moura [a,b], Ana Godinho-Santos [a,b], Rita T. Marques [a,b], André MC Gomes [a,b], Cristina Ferreira [a,b,c], Helena Nunes-Cabaço [a,b], Perpétua Gomes [d,e], José Poças [f], Carlos Vasconcelos [g,h], Robert Badura [a,b,c], Ana E. Sousa [a,b,*]

[a] GIMM - Gulbenkian Institute for Molecular Medicine, 1649-028 Lisbon, Portugal
[b] Faculdade de Medicina, Universidade de Lisboa, 1649-028 Lisboa, Portugal
[c] Hospital de Santa Maria, Unidade Local de Saúde de Santa Maria, 1649-035 Lisboa, Portugal
[d] Egas Moniz Center for Interdisciplinary Research (CiiEM), Egas Moniz School of Health & Science, 2829-511 Caparica, Portugal
[e] Laboratório de Biologia Molecular, SPC, Unidade Local de Saúde Lisboa Ocidental, Hospital Egas Moniz, 1349-019 Lisboa, Portugal
[f] Serviço de Infecciologia, Hospital de São Bernardo, Unidade Local de Saúde da Arrábida, 2910-446 Setúbal, Portugal
[g] Imunologia Clínica, Hospital de Santo António, Unidade Local de Saúde de Santo António, 4099-001 Porto, Portugal
[h] Unidade Multidisciplinar de Investigação Biomédica (UMIB), Instituto de Ciências Biomédicas Abel Salazar (ICBAS), Universidade do Porto, 4050-313 Porto, Portugal

ARTICLE INFO

Article history:
Accepted 8 May 2026
Available online 14 May 2026

Keywords:
HIV
HIV-2
Lymph nodes
Germinal centre
T lymphocytes
Virus replication

SUMMARY

HIV-2 infection is associated with low-to-undetectable plasma viral load, broad and sustained specific antibody and T cell responses, and a slow course of CD4 T cell decline, even in the absence of antiretroviral therapy (ART). Here, we investigated the secondary lymphoid organs of people with HIV-2 (PWH2) as compared to people with HIV-1 (PWH1) and seronegative subjects. We found active HIV-2 replication and major disruption of lymph node architecture in PWH2, also attested by the alterations that we demonstrated in the blood counterparts of follicular T and B cells. These findings were corroborated by in vitro infection assays using tonsil organ cultures and HIV-2 or HIV-1 primary isolates with distinct co-receptor usage, CCR5 or CXCR4, which showed significant HIV-2 cytopathogenicity associated with post-transcriptional control of HIV-2 replication, revealed by high titres of cell-associated viral DNA and mRNA transcripts but reduced HIV-2 protein production. Overall, our findings support a major impact of HIV-2 on secondary lymphoid tissue organisation throughout the disease course, stressing the relevance of this neglected infection to understand host-pathogen equilibrium in retroviral zoonoses and to identify strategies towards a functional HIV cure.

Introduction

Lymph nodes are the main sites of HIV replication and for the mounting of specific immune responses.[1,2] Lymph node architecture and function also determine lymphocyte homeostasis and HIV disease progression.[1,3] Nevertheless, the lymph node pathology associated with naturally occurring HIV-2 infection, the non-pandemic form of HIV/AIDS, remains poorly characterised.[4–6]

HIV-2 disseminates and establishes viral reservoirs similarly to HIV-1,[6–9] and, notably, follicular helper T cells (TFH) are also key HIV-2 reservoirs.[10] Notwithstanding this, viremia is typically low to undetectable in people with HIV-2 (PWH2) before the initiation of antiretroviral therapy (ART).[7,11] The reduced plasma viral load explains the low transmission rates and the confinement of HIV-2 infection to West Africa and related countries like Portugal,[4,11] and the prediction of its progressive decline in countries even without access to ART.[12] Importantly, untreated PWH2 feature a slow progressive disease with limited impact on survival,[13,14] despite systemic inflammation and the observed direct correlation between CD4 decline and upregulation of immune activation markers, as in PWH1.[11] HIV-2-specific responses were shown to be polyfunctional and

* Corresponding author at: GIMM - Gulbenkian Institute for Molecular Medicine, 1649-028 Lisbon, Portugal.
E-mail addresses: asousa@medicina.ulisboa.pt, ana.e.sousa@gimm.pt (A.E. Sousa).

https://doi.org/10.1016/j.jinf.2026.106760

maintained throughout the disease course, encompassing both neutralising antibodies (nAbs)[15–18] and helper[19,20] and cytotoxic[21,22] T cell responses. Therefore, HIV-2 has been explored as a model for a functional HIV-1 cure.[5,23–25]

Several findings support an impact of HIV-2 on lymph nodes and germinal centres (GCs). The nAb titre correlated with a contraction of the circulating memory B cell compartment,[26] and a loss of both switched and unswitched memory B cells was found in PWH2 as compared to both PWH1 and seronegatives.[27] HIV-2 infection also induces CD4 cell tropism to lymph nodes,[6] and generalised lymphadenopathy.[14,25,28–30] However, it remains unclear whether it follows the histologic patterns described in PWH1, namely, follicular hyperplasia followed by progressive follicular involution and diffuse effacing of the lymph node organisation with GC disruption and lymphocyte depletion at AIDS.[1] We investigated here the impact of HIV-2 in the lymph nodes and in the circulating follicular T cell compartment of PWH2.

Patient and methods

Human samples

This work gathered rare samples of PWH2 living in Portugal, the non-African country with the highest HIV-2 prevalence.[11,31] After a multicentric retrospective study of archived lymph node samples from Portuguese hospitals excluding cases of tuberculosis or neoplasia, we identified 3 biopsies from cervical lymph nodes of ART-naïve PWH2, namely: i) 55 y female (744 CD4 T cells/µl, 7278 HIV-2 RNA cps/mL, Hospital de São Bernardo, Setúbal) with lymphadenopathy and fever, who subsequently started ART and remained asymptomatic for the 13 y follow-up; ii) 58 y female (255 CD4 T cells/µl, undetectable viremia, Hospital de Santa Maria (HSM), Lisbon) who developed lymphadenopathy 6 y after the diagnosis of HIV-2 infection, started ART 3 y after the biopsy, and remained asymptomatic for the 22 y follow-up; and iii) 46 y male (73 CD4 T cells/µl, undetectable viremia, Hospital Santo António, Porto) with fever and generalized lymphadenopathy, irregular follow-up, poor adherence to ART, with death occurring within 1 y after the lymph node biopsy. These biopsies were compared with those collected at HSM, from 12 PWH1 in the workup of lymphadenopathy with the final pathology diagnosis of reactive lymphoid hyperplasia (9 with male sex assigned at birth, age range 36–66 y with a median of 53 y, median CD4 T cell counts of 328 cells/µl with limits 50–610 cells/µl, median viremia 5580 RNA cps/mL with limits 27–43400 RNA cps/mL, which was undetectable in the 4 out of the 9 patients under ART before the biopsy), and from 7 seronegative individuals mainly collected during elective surgery (4 with male sex assigned at birth, age range 26–85 y with a median of 66 y). Peripheral blood samples were collected from 20 PWH2 and 19 PWH1 under follow-up at HSM, and 21 age-matched seronegative subjects, whose clinical and epidemiological features are depicted in Table 1. Buffy-coats were obtained from blood donors through the Instituto Português do Sangue e Transplantação (IPST). HIV-2 viremia was quantified at the Molecular Biology Laboratory in Egas Moniz Hospital, Lisbon, Portugal.[32] Tonsil tissue specimens were obtained during routine paediatric tonsillectomy performed at HSM. All participants or their legal representatives provided written informed consent. The study was approved by the ethical board of the Centro Académico de Medicina de Lisboa (CAML), and the ethical boards of the other above-mentioned hospitals.

Immunohistochemistry

Archived lymph node biopsy specimens were all formaldehyde-fixed and paraffin-embedded (FFPE). Three-micrometre tissue sections were obtained using a Leica microtome (RM2145). Sections for single immunohistochemistry staining were deparaffinized and submitted to heat-induced epitope retrieval (HIER). Samples were stained with the following antibodies to identify different cell subsets (clone and supplier in brackets): anti-CD3 for T cells (F7.2.38, Dako), anti-CD4 for helper T cells (SP35, Cell Marque), anti-CD8 for cytotoxic T cells (1A5, Leica), and anti-IgD (DRN1C, Leica) for B cells, anti-CD21 for follicular dendritic cells and B cells (1F8, Dako), anti-CD68 for macrophages (PG-M1, Dako), anti-Foxp3 for regulatory T cells (236/E7, eBioscience). Staining was revealed with DAB (3,3'-diaminobenzidine) oxidation (brown) by horseradish peroxidase (HRP). Double immunohistochemistry staining, using anti-CD4 (SP35, Cell Marque) and anti-Ki67 (B56, BD) to identify cycling CD4 T cells, was performed using the Ventana BenchMark ULTRA automated system and revealed through Fast Red (with alkaline phosphatase) and DAB (by HRP) oxidation (red and brown, respectively). All slides were counterstained with Harris' Haematoxylin (Bio-Optica) and mounted with Quick-D mounting medium (Klinipath) for single staining, or Glycergel (Dako) for double staining. Haematoxylin-eosin (H&E, histological architecture) and Gomori (reticulin network) stains were blindly evaluated by a trained pathologist and scored according to their degree of architectural damage. Samples infected with HIV-1 and HIV-2 were stained with anti-p24 (KAL-1, Dako) or anti-p27 (MAb ARP396/397; P. Szawlowski, NIBSC, Centre for AIDS Reagents, Medical Research Council [MRC]), respectively, incubated with a peroxidase-diaminobenzidine detection system (EnVision; Dako), and counterstained with Harris's Haematoxylin (Bio-Optica). Additionally, in situ hybridization (ISH) targeting HIV mRNA was performed using the chromogenic single-plex RNAscope™ 2.5 HD Assay BROWN (#322370, Bio-Techne) for archived FFPE lymph node samples from PWH2 and PWH1, both with antisense probes for gag-pol mRNA, namely a catalogue probe for HIV-1 (Probe-HIV-gagpol, #317691, Bio-Techne) and a custom-made probe for HIV-2, built for a consensus of preserved gag-pol regions (Probe-V-HIV2-gagpol-C1, #1108531-C1, Bio-Techne). Samples were first assessed for RNA preservation using a positive control probe for PPIB (peptidylprolyl isomerase B) housekeeping gene and specificity of probe binding was compared with a negative control probe for bacterial dapB (dihydrodipicolinate reductase gene of *Bacillus subtilis*).

Image analysis of lymph nodes

Whole slide imaging with Hamamatsu NanoZoomer-SQ Digital Slide Scanner was performed for H&E, Gomori, immunohistochemistry and RNAscope stainings. Images were scanned at 400X optical magnification (with digital magnification up to 800X). Image screening and analysis was done with NDP.view2 software (v2.9.29). For germinal centre circularity analysis, the whole-slide images were analysed with Fiji/ImageJ software (version 1.52k). An object mask was generated for each lymph node, using the CD21 staining as the colour threshold for germinal centre mapping. GC Shape quantification was obtained using the tool Shape Discriminator Maps from BioVoxxel Toolbox© (BioVoxxel_Plugins-2.0.1, Jan Brocher).

Analysis of HIV infection of tonsil organ cultures (TOCs)

Tonsil tissue pieces were placed on Millicell cell culture inserts (Millipore) in a 6-well plate containing 1250 µl of TOC medium (complete medium with 15%FBS, 1 mM sodium pyruvate, and 1% minimal essential medium nonessential amino acids [all from Gibco]). A third of the medium was replaced every 2 to 3 days. HIV infection was performed by placing a 5 µl drop containing 3 ng RT of virus on top of each TOC. The following viruses were used: HIV-$1_{92US660}$ and HIV-$2_{60415\ K}$ (both CCR5 tropic), as well as HIV-$1_{92HT599}$ (CXCR4 tropic) provided by the Multicenter AIDS Cohort Study, NIH

Table 1
Clinical and epidemiological data of the cohorts for the ex vivo blood studies.

	Seronegative	PWH2	PWH1
Numbers [male/female]	21 [11/10]	20 [3/17]	19 [9/10]
Age, years	51 ± 2.1 (33–65)	**59 ± 2.7 (34–76)***	**54 ± 2.6 (25–73)**
Ethnicity, caucasian/other	21/0	4/16	14/5
Time on ART, years	NA	**6.6 ± 1.5 (1–20)**§	**11.5 ± 1.8 (1–24)**
% CD4 T cells	48.3 ± 1.8 (36.7–63.5)	**31.5 ± 2.5 (16.0–56.8)*****	**24.9 ± 1.6 (12.5–41.2)*****
CD4 T cells/µl	1154 ± 93 (642–2703)	**565 ± 56 (164–1115)*****	**509 ± 40 (224–843)*****
% CD8 T cells	22.9 ± 1.3 (8.3–31.9)	**33.1 ± 2.4 (11.6–56.2)****§§	**46.9 ± 2.9 (28.3–81.6)*****
CD8 T cells/µl	546 ± 45 (174–901)	**594 ± 71 (278–1470)**§§	**980 ± 100 (445–2363)*****
CD4/CD8	2.38 ± 0.28 (1.26–6.91)	**1.13 ± 0.15 (0.29–2.80)*****§§	**0.59 ± 0.06 (0.15–1.09)*****
TFH cells/µl	183 ± 17 (77–405)	**86 ± 9 (31–195)*****	**95 ± 13 (38–258)*****
TFR cells/µl	28 ± 3 (10–60)	**10 ± 2 (2–27)*****	**11 ± 1 (3–24)*****
TFC cells/µl	10 ± 2 (3–39)	**17 ± 3 (5–56)***	**26 ± 5 (5–85)****
ESR, mm	NA	47 ± 9 (5–120)	27 ± 7 (2–120)
C reactive protein, mg/dL	NA	0.49 ± 0.13(0.04–2.52)	0.36 ± 0.09 (0.05–1.63)
IL-6 pg/mL	NA	5.16 ± 1.02(1.50–22.00)	5.87 ± 2.28 (1.60–46.10)
D-dimers, µg/mL	NA	**0.83 ± 0.13 (0.15–2.15)**§§	**0.34 ± 0.04 (0.19–0.76)**
β2m, mg/L	NA	2.93 ± 0.61 (1.32–13.47)	2.53 ± 0.33 (1.31–7.36)
Ferritin, ng/mL	NA	133 ± 20 (20–299)	157 ± 44 (24–784)
TG; mg/dL	NA	107 ± 7 (58–180)	116 ± 14 (14–250)

Data are Mean ± SEM with limits in brackets (min-max), unless otherwise indicated. NA, not applicable. Data were compared using Mann-Whitney test. Statistical differences between a given PWH cohort and seronegative controls:
*, $p < 0.05$
**, $p < 0.01$
***, $p < 0.001$.
Statistical differences between PWH1 and PWH2:
§, $p < 0.05$
§§, $p < 0.01$
Reference values for ESR: < 20 mm; C reactive protein: < 0.5 mg/dL; IL-6 < 1.5 pg/dL; D-dimers: 0.0-0.5 µg/dL, β2m (β2 microglobulin): 0.8-3.0 mg/dL; ferritin: 13-150 ng/mL TG (triglycerides): < 150 mg/dL.

AIDS Reagent Program, Division of AIDS, NIAID, NIH; HIV-$2_{20.04}$, previously represented as PTHCC20/2004 and 19/2004, kindly provided by Nuno Taveira.[10,33] Viral stocks were propagated in pools of isolated peripheral blood mononuclear cells (PBMCs) stimulated for 3 days with phytohemagglutinin (PHA; 5 µg/mL; Sigma) and maintained with human recombinant interleukin-2 (IL-2;10 U/mL; from Maurice Gately, Hoffman-La Roche Inc., through the NIH AIDS Reagent Program), as described previously.[33] Virus in cell-free culture supernatants was quantified by measuring reverse activity (RT) using SYBR Green Product-Enhanced RT (SG-PERT), previously described.[10,33] On day 7, TOCs were mashed and the obtained cell suspensions stored as cell pellets at −80 ºC, for viral readouts and immediately analysed by flow cytometry. Surface staining was performed for 20 min at room temperature, including fixable viability dye (eBioscience) for dead cell exclusion. Cells were subsequently fixed, permeabilized and intracellularly stained using the Foxp3 staining kit (eBioscience), as described previously,[33] using the anti-human monoclonal antibodies (mAbs) listed in S1 Table, see supporting information. Gag protein production was quantified using KC57 (Beckman Coulter), an antibody that detects both HIV-1 and HIV-2 Gag.[2] Cells were acquired at a LSRFortessa (BD Biosciences) and data were analysed using FlowJo Software (V10.4, TreeStar).

TFH differentiation assay in the presence of HIV-2 or HIV-1

PBMCs were isolated from buffy coats (BC) from blood donors (Instituto Português do Sangue e Transplantação, IPST) via Ficoll-Paque (Cytiva), and naïve CD4 T cells were purified (> 85% purity) by magnetic negative isolation (Human CD4 Naïve T Cell Isolation Kit, MojoSort; BioLegend). Naïve CD4 T cells were labelled with Cell Trace Violet™ (CTV, Invitrogen), and T cell receptor (TCR) stimulated (1:4 DynaBeads Human T-activator CD3/CD28, Life Technologies) overnight. After washing to remove stimuli, cells were incubated for 4 h with 235 PFU of dual-tropic viruses HIV-1 92/US/723 or HIV-2 CBL-23 primary isolates (from NIH AIDS Reagent Program). Cells were subsequently cultured with immobilized anti-CD3 (5 mg/mL Clone OKT3, eBioscience) and soluble anti-CD28 (1 mg/mL Clone CD28.2, eBioscience) and supplemented with an optimized mix of human recombinant cytokines known to promote TFH differentiation,[34] namely IL-12 [10 ng/mL] + IL-1β [10 ng/mL] + IL-6 [25 ng/mL] + TGF-β [5 ng/mL] (all from PeproTech). In parallel, stimulated cells and unstimulated cells were cultured with IL-2 [10 U/mL] and used as controls. After 72 h (day 5), TCR stimuli was removed, and cells were resuspended in fresh medium supplemented with either the cytokine mix or IL-2 and maintained in culture for additional 48 h (day 7). Cells were collected at days 5 and 7, stored at −80 ºC for viral readouts and immediately analysed by flow cytometry. Surface and intracellular staining were performed using the antibody panels listed in S2 Table, see supporting information, and previously described protocols.[10] Samples were acquired in a 3-laser spectral flow cytometer Aurora (Cytek Biosciences) and analysed using FlowJo Software (V10.4, TreeStar). Gated cells were exported as FCS files into R (v4.1.2; R Foundation for Statistical Computing) and unsupervised analysis performed as described below for the analysis of blood samples.

Flow cytometry analysis of blood samples

After erythrocyte bulk lysis, whole-blood samples (5 M cells/tube) were incubated with FcR blocking reagent (Miltenyi Biotec) for 15 min at 4ºC. Staining was performed with antibodies listed in S3 Table, for 30 min at RT, and fixed with FACS Lysing solution (BD Biosciences) at RT. PBMCs (2 M cells/tube), purified from heparinized blood after a Ficoll-Paque (Cytiva) density centrifugation, were incubated with surface antibodies and FcR Blocking Reagent for 25 min at RT and subsequently fixed and permeabilized with Fixation/Permeabilization Buffer (eBioscience) for 30 min at 4ºC. Cells were then stained for 30 min at 4ºC with the intracellular antibodies listed in Supplementary Table 3. After fixation, all samples were immediately acquired in a spectral flow cytometer Aurora (Cytek Biosciences). Manual compensation was performed on SpectroFlo® (version 3.0.1) and FCS files were exported. The following gating strategy was applied (FCS Express, v7.14.0020), lymphocytes were gated based on forward and side scatter, as well as

doublets exclusion. T cells were gated as $CD45^{+}CD3^{+}CD19^{neg}GD^{neg}$, B cells were gated as $CD45^{+}CD3^{-}CD19^{+}$. Gates were exported as FCS files and imported into R (v4.1.2). Arcsinh transformation was applied to all files with flowVS (v1.34.0), followed by cleaning with FlowAI (v1.32.0) and normalization based on landmark registration with warpSet function from flowStats package (v4.14.1). Transformed and normalized expression values were exported into fcs files with the FlowCore package. UMAP was used as a dimensional reduction method, based on the expression levels of all markers except the ones used for the previous gating. FlowSOM (CATALYST package, 1.26.0) was applied as clustering method. Clusters that here present only in some individuals were merged, to avoid over clustering.

Quantification of HIV DNA and mRNA by real-time PCR

DNA and RNA were extracted from cell pellets using the ZR-Duet DNA/RNA MiniPrep Kit (Zymo Research) according to the manufacturer's instructions. For *gag* mRNA quantification, 50 ng of total RNA was used to synthesise cDNA using oligo(dT)20 and Superscript III®RT (Invitrogen) as described previously.[10,33] Real-time PCR was performed using TaqMan® Gene Expression Master Mix (Applied Biosystems) with the primers and probes described in S4 Table, see supporting information. Standard curves were generated from serial dilutions of cDNA prepared from the mRNA of PBMCs of 3 different healthy individuals (for GAPDH [glyceraldehyde-3-phosphate dehydrogenase] quantification) or plasmids containing the amplicons of HIV-1 *gag* and CD3ϒ (a kind gift from Rémi Cheynier) or of HIV-2 *gag*, described previously.[10,33] Quantification was performed using an Applied Biosystems 7500 Fast real-time PCR system.

Statistical analysis

Statistical analysis was performed using Graph-Pad Prism (v9.5.0, GraphPad Software) and R. For R, the ggpubr package (v0.6.0) was used for statistical testing and ggplot2 (v3.5.1) for data visualisation. For the lymph nodes data, the analysis was performed using IBM SPSS Statistics 21 Software. Data were compared using one-way ANOVA or Kruskal-Wallis was used to compare groups, and for post-hoc comparisons, Bonferroni's and Dunn's tests were applied using the Holm-Bonferroni correction. p values ≤ 0.05 were considered significant.

Results

Active viral replication and CD4 depletion in lymph nodes from PWH2

We performed a retrospective study of FFPE lymph nodes archived in major Portuguese hospitals, and, after excluding opportunistic infections and tumours, we identified 3 samples from ART naïve PWH2 at distinct disease stages, as assessed by the degree of circulating CD4 T cell depletion, to investigate viral replication and histologic alterations. As expected for PWH2,[7,11] viremia was undetectable or below 10,000 RNA cps/mL. Notwithstanding this, we identified cells that stained positive for anti-p27 in all lymph nodes (Fig. 1A), using an antibody for SIV Gag known to cross-react with HIV-2 Gag.[33,35] Moreover, in the two PWH2 with higher CD4 T cell counts, the RNA was sufficiently well-preserved in the FFPE biopsies to allow the evaluation of *gag* mRNA by RNAscope, allowing us to document active viral transcription in both cases (Fig. 1B). We then asked whether the ongoing viral replication was associated with CD4 T cell depletion in the non-germinal centre (GC) areas of the lymph nodes. For this purpose, these samples were matched for age and peripheral blood CD4 T cell counts to lymph node biopsies from 12 PWH1, and 7 seronegative individuals (Fig. S1A and S1B). We found a decrease in the area stained for CD4 in the lymph nodes from PWH2 in parallel to the decline in peripheral blood CD4 T cell counts (Figs. 1C and 1D), which was accompanied by only a slight relative increase in the proportion of the area stained for CD8, as compared to PWH1 (Figs. 1C and 1D, see also S1A). Notably, PWH2 featured no decrease in percentages of the non-GC area that stained positive for Foxp3, a marker for regulatory T cells (Tregs), as compared to both PWH1 and seronegative individuals (Figs. 1C and 1D, see also S1A). Moreover, the ratio of CD4+/Foxp3+ stained areas was below the median observed in seronegatives and in PWH1 grouped by circulating CD4 T cell counts (Fig. 1D).

Overall, our findings support a progressive decline in CD4 T cells in the non-GC regions of the lymph nodes of PWH2 in line with the degree of peripheral blood depletion. Moreover, the data suggest a better preservation of Tregs and less pronounced CD8 T cell expansion than in PWH1, despite the evidence of cells with active HIV-2 replication.

Germinal centre disruption in lymph nodes from PWH2

Next, we focused our analysis on the GC areas of the lymph nodes from PWH2. Significant GC disruption was found irrespective of the staining approaches (Fig. 2A), namely: structure evaluation (HE and reticulin/Gomori), B cells (CD21, IgD), cell proliferation (CD4/Ki67), CD8+ cell infiltration, follicular regulatory T cells (Foxp3) and macrophage distribution (CD68). The GC disruption is particularly marked in the PWH2 with 73 CD4 T cells/μl but was already observed in the PWH2 with preserved circulating CD4 T cell counts (Fig. 2A). In this context, it was not possible to develop algorithms to quantify stained areas, but the disruption appears to be more marked than in the lymph nodes from 3 PWH1 with comparable degrees of depletion of circulating CD4 T cells (Fig. 2A). Additionally, we used the CD21 staining to evaluate the area and shape of the GC in the lymph nodes, as shown in Fig. 2B, as a quantitative estimation of the disruption of the lymph node architecture, rather than a functional evaluation. The estimated values showed a loss of circularity of the GC in the lymph nodes of PWH2, more marked or comparable to the worst cases observed in lymph nodes from PWH1 (Fig. 2B).

Thus, our analysis of these 3 lymph nodes from PWH2 with a wide range of blood CD4 T cell counts indicated that HIV-2 infection may induce major GC disruption.

HIV-2 replicates in tonsil organ cultures and depletes TFH

To further investigate the impact of HIV-2 infection in lymphoid tissues, we established an in vitro infection system using fresh tonsil tissue (TOC, Fig. 3A), which has been shown to support infection in the absence of exogenous stimuli.[36,37] We selected both HIV-2 and HIV-1 primary isolates with known co-receptor usage, CXCR4 or CCR5, that have been used in our previous studies to investigate HIV infection both in the human thymus[33] and in purified TFH from human tonsils.[10]

We found that all isolates were able to infect the tissue as assessed by cell-associated viral DNA and viral mRNA, as well as intracellular Gag protein staining in the cell suspensions (Fig. 3B). Although the levels of total viral DNA and mRNA did not show significant differences between HIV-1 and HIV-2, as well as CXCR4- and CCR5-using isolates, there was a clear trend to higher levels in HIV-1_{X4} than in HIV-1_{R5}, which was not observed with the HIV-2 isolates. (Fig. 3B). In agreement, the proportion of CD4 T cells positive for Gag protein was significantly higher in HIV-1_{X4} than in all the other isolates (Fig. 3B, see also S2A and S2B). This finding was in line with our previous data showing a posttranscriptional control of HIV-2 production upon in vitro infection of human thymocytes,[33] a process that was subverted in the infection of stimulated PBMCs.[33] Importantly, both HIV-2_{X4} and HIV-1_{X4} induced comparable levels of cell death and CD4 loss, which were significantly higher than in the

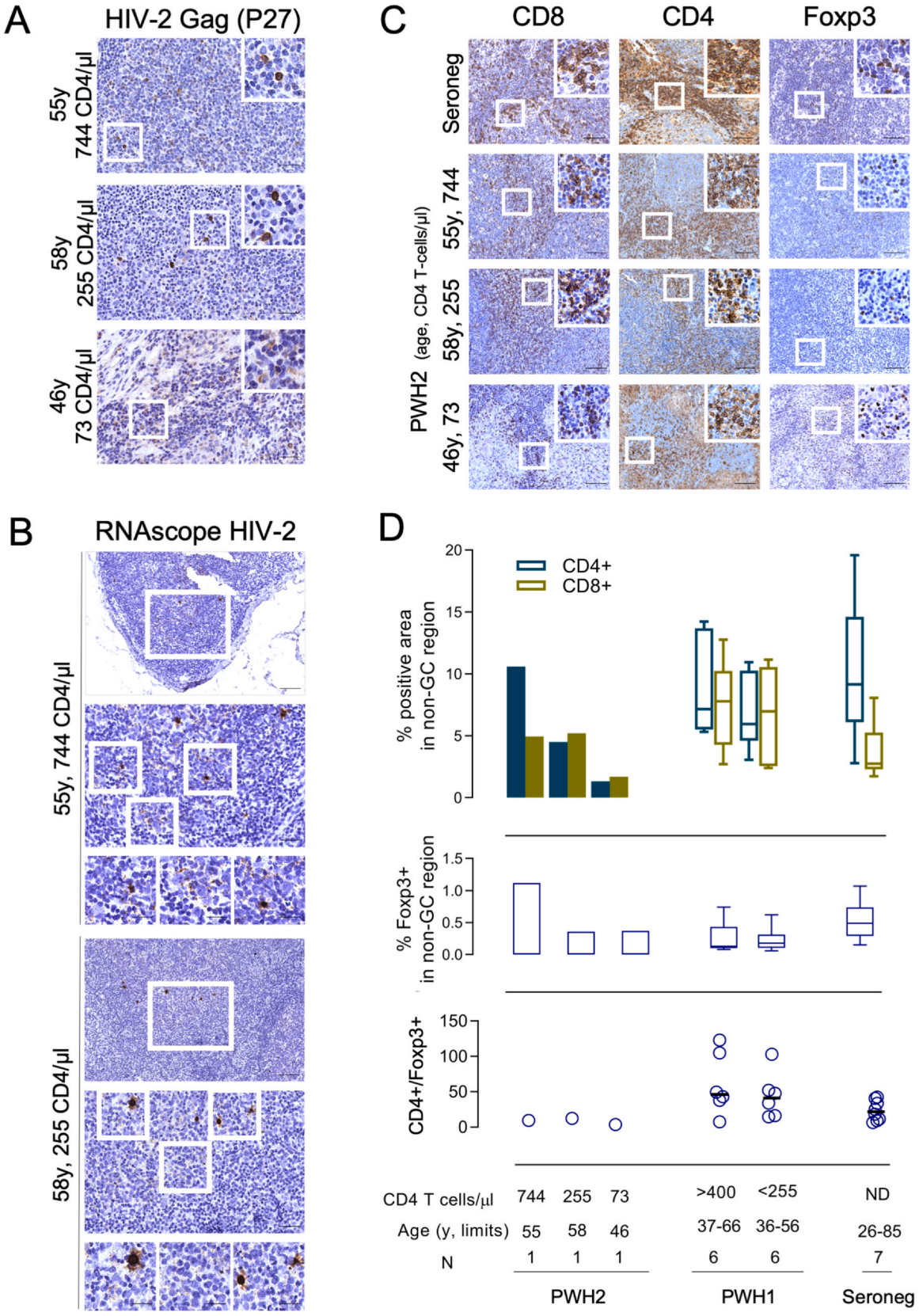

(caption on next page)

Fig. 1. CD4 T cell depletion in non-GC areas and viral production in lymph nodes from PWH2. (A) Micrographs show immunohistochemistry staining (200X) of lymph nodes using anti-p27 (ARP396/397, NIH); Amplifications (400X) of each selected area are shown in the right of each picture; Scale bar = 100 µm. (B) HIV-2 gag mRNA expression (brown) evaluated by RNAscope 2.5HD Assay (100X, black bar = 250 µm), with a custom probe (Probe-V-HIV2-gagpol-C1, #1108531-C1, Bio-Techne) and haematoxylin for contrast staining (blue). Amplifications of 200X (Scale bar = 100 µm) and insets at 400X (Scale bar = 50 µm). (C) Micrographs show immunohistochemistry staining (200X) of CD8, CD4 and Foxp3 in the non-GC area of lymph nodes from PWH2 and a representative seronegative subject. Inset in the left upper quadrant shows an amplification (400X) of the white square area. Scale bar = 100 µm (D) Quantification of the non-GC area stained for CD4 (blue) and CD8 (green) in the top graph, Foxp3 in the middle graph, and the ratio of areas stained for CD4 and Foxp3 in the bottom graph in PWH2, as well as in PWH1 grouped accordingly to the blood CD4 T cell counts (> 400 cells/µl, n=6; < 255 cells/µl, n=6) and the grouped seronegative individuals (n=7). Graphs show median and interquartile range. Numbers below refer to blood CD4 T cells/µl and age; ND – not done. Boxplots represent the median and interquartile range. Bars represent the mean. No significant differences were found.

case of infections with HIV-2_{R5} or HIV-1_{R5} (Fig. 3C). Notably, none of the isolates induced significant loss of Foxp3+ Tregs (Fig. 3C).

We next asked whether germinal centre cells were preferentially targeted by HIV-2 infection. For this purpose, the cell suspensions generated from TOCs on day 7 post-infection were stained with CXCR5 and PD-1 and analysed as illustrated in Fig. S2A and S2B. All virus isolates induced a significant loss of TFH, even though the depletion was more marked in CXCR4-using viruses (Fig. 3D). There were no significant differences between HIV-2 and HIV-1 isolates using the same co-receptor (Fig. 3D). Notably, the follicular CD4 T cells expressing Foxp3 (TFR) were better preserved (Fig. 3E), and there was no loss of follicular CD8 T cells (TFC) in all the infection conditions (Fig. 3F).

Overall, this model of short-term infection of lymphoid tissue revealed a major impact of HIV-2 infection with follicular T cells as the main targets.

Preserved TFH differentiation from naïve cells infected with HIV-2

Next, we compared the impact of HIV-2 or HIV-1 on TFH differentiation in vitro using an assay developed by Ueno.[34] Naïve CD4 T cells were sort-purified from the peripheral blood of healthy donors and infected with dual-tropic HIV-2 or HIV-1 primary isolates to circumvent the impact of co-receptor usage, as outlined in Fig. 4A. Comparable levels of cell-associated total DNA were found at 72 h post-infection / day 5 (Fig. 4B). Notably, the profile of increase of the frequency of CXCR5+ cells, a global TFH estimate, was comparable in the presence of HIV-2 or HIV-1, with no apparent impact at day 5 and 7 (Fig. 4C, see also S3A). Additionally, we applied an unsupervised approach (UMAP) to analyse the kinetics of expression of a panel of markers associated with TFH function (Bcl-6, PD-1, ICOS, OX40, CD57) and general markers of cell activation/differentiation (CD45RA/RO, CD69, CD25, Foxp3, CCR6, CXCR3) along the culture. We have also evaluated SAMHD1 expression, given its interplay with BCL-6 in TFH differentiation,[38] and the ability of the HIV-2 protein Vpx to overcome its restriction and facilitate HIV infection in quiescent naïve cells.[39,40]

As shown in Fig. 4D, the main determinant of the UMAPs was the donor of the naïve cells, as the evolution patterns were similar between the infection conditions. The detailed phenotype of the generated CXCR5+ cells confirmed the lack of significant impact of HIV-2 infection (Fig. 4E, see also S3B and S3C for comparison between day 5 and day 7 and additional markers).

Therefore, despite harbouring Vpx, the addition of HIV-2 to an in vitro assay of TFH differentiation from naïve CD4 T cells did not affect yields or final TFH phenotype.

Perturbed circulating follicular compartment in PWH2

These findings prompted us to pursue the investigation of circulating CXCR5+ T cells from PWH2, which are more accessible counterparts of germinal centre follicular cells.[41] We applied a comprehensive spectral flow cytometry panel of markers of TFH differentiation and immune activation to freshly collected blood from 60 subjects (Table 1). Both PWH2 and PWH1 featured undetectable viremia under ART with comparable CD4 T cell counts, but CD8 T cell counts were significantly higher in PWH1 (Table 1).

The analysis of CXCR5+ cells revealed a significant decrease in TFH (CXCR5+Foxp3^{neg}CD4+) and TFR (CXCR5+Foxp3+CD4+) with an expansion of TFC (CXCR5+CD8+) in both PWH2 and PWH1 when compared to seronegative individuals (Fig. 5A and Table 1).

The unsupervised analysis of TFH revealed a relatively similar pattern of alterations in PWH, irrespective of virus type, when compared to seronegative (Fig. 5B). Both PWH2 and PWH1 featured significant: 1) underrepresentation of the cluster TFH11 (CXCR3^{neg}CCR6^{neg}CCR4^{neg}PD1^{neg}); 2) overrepresentation of the clusters TFH1, TFH15, and TFH16, expressing the proliferating marker Ki67 and PD-1, with variable levels of CXCR3, CCR6, and HLA-DR; 3) overrepresentation of the cluster TFH6, showing a memory stem-cell like phenotype, namely lack of CD45RO in the presence of CD95 and CXCR3 (Fig. 5B). The only significant difference was a lower expansion of cluster TFH12, expressing Ki67 without markers of differentiation, in PWH2 than in PWH1 (Fig. 5B).

PWH2 also showed a profile of TFR alterations comparable to those found in PWH1 (Fig. 6A), with a significant overrepresentation of the TFR clusters 1 and 3–6, expressing Ki67, and underrepresentation of the cluster TFR2 with a naïve-like phenotype (Fig. 6A).

Although our panel was designed to evaluate TFH and TFR, the unsupervised analysis of TFC identified distinct profiles in the 3 groups with significant differences between PWH2 and PWH1 (Fig. 6B). The cluster TFC1 with stem-cell memory profile (CD45RO^{neg}CD95+CCR7+CD127+CD31+CXCR3+CCR6^{neg}) was significantly expanded in PWH2 compared with both PWH1 and seronegative individuals (Fig. 6B). Moreover, PWH1 featured an overrepresentation of the cluster TFC8, expressing PD1, and an underrepresentation of the cluster TFC7, expressing HLA-DR, CD39 and CXCR3, compared with PWH2 and seronegative (Fig. 6B), supporting differences in cytotoxic function that deserve future functional evaluation.

Overall, PWH2 featured major alterations in circulating CXCR5+ T cells in agreement with persistent alterations in lymph nodes. Additionally, we showed that there were also imbalances in circulating B cells, further supporting the GC disruption (Fig. S4A and S4B). The unsupervised analysis of blood B cells revealed significant overrepresentation of clusters B10 and B11 (both CD21lowCD38low) and underrepresentation of cluster B4 (unswitched memory) in PWH2 as compared to seronegative individuals (Fig. S4A and S4B). Moreover, cluster B7 (switched memory) was significantly smaller in PWH2 than in PWH1 and seronegative (Fig. S4A and S4B), in agreement with our previous reports in other cohorts.[26,27] Of note, the serum levels of IgG4 were also lower in PWH2 than in PWH1 (Fig. S4C), further supporting a sustained perturbation of germinal centre responses.[42,43]

Altogether, the ex vivo analysis of circulating follicular T cells and B cells from PWH2 revealed a major impact of HIV-2 on germinal centres, in line with the alterations observed in the lymph nodes from PWH2 and upon HIV-2 infection of tonsil organotypic cultures.

Discussion

We show here that the relatively benign course of HIV-2 infection is linked to remodelling of the secondary lymph nodes, supported by both direct evidence from lymph node biopsies of PWH2

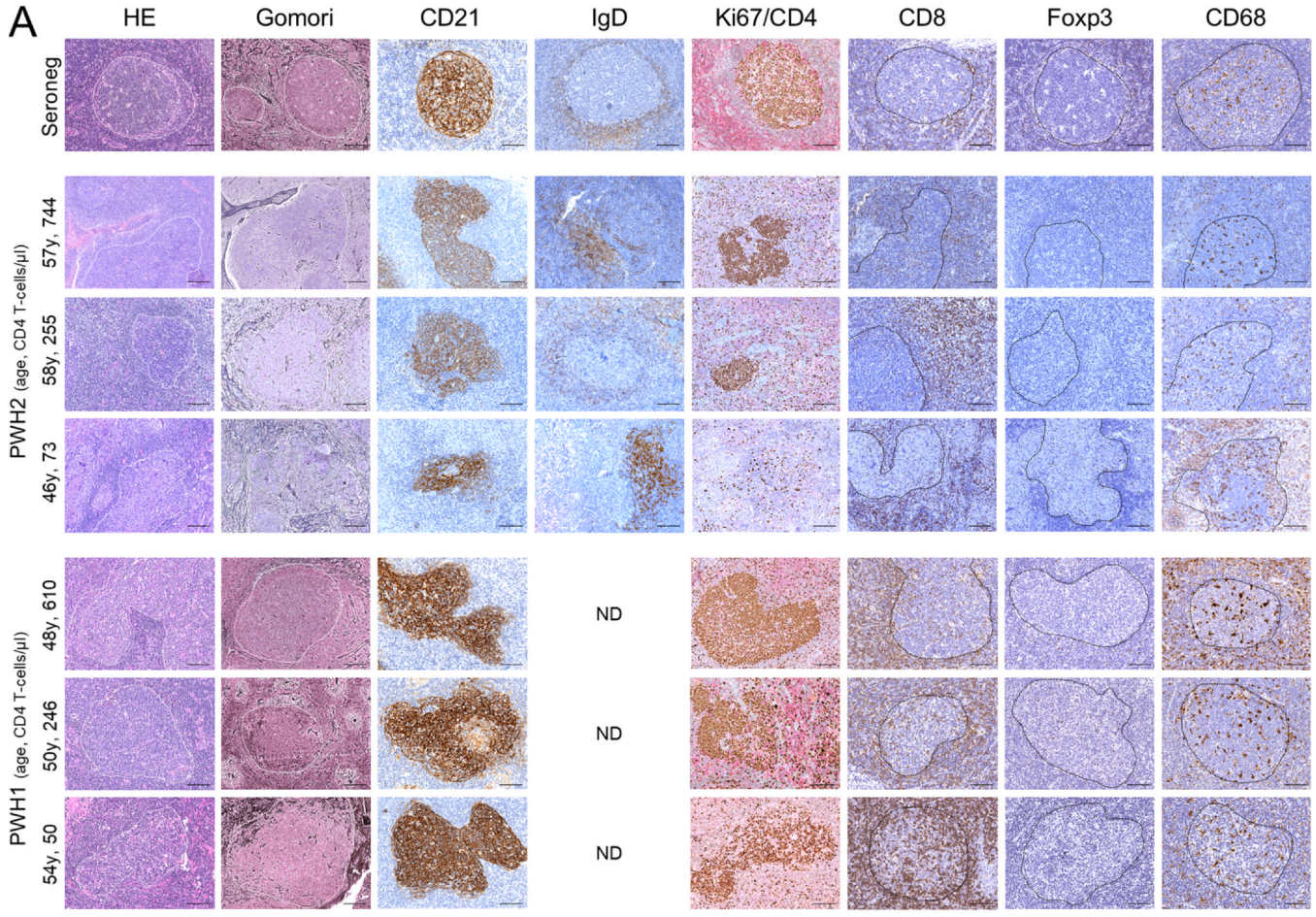

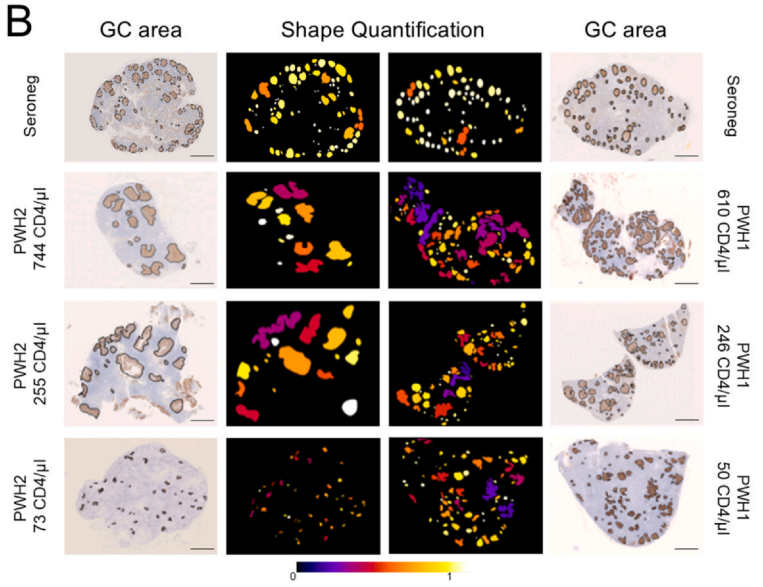

Fig. 2. Germinal centre disruption in lymph nodes from PWH2. (A) HE, Gomori, CD21, IgD, Ki67 (brown)/CD4(red), CD8, Foxp3 and CD68 staining of GC areas from PWH2, PWH1 (matched for blood CD4 T cells/µl and age) and a representative seronegative, from left to right, respectively (Magnification 200X; Scale bar = 100 µm; ND – not done). (B) Representative images of computer analysis for circularity of GCs defined by CD21 staining in lymph nodes from PWH2 and PWH1 paired for the degree of blood CD4 T cells, as well as representative seronegatives (Magnification 84X; Scale bar = 2500 µm); colour scale estimates circularity in which white colour represents value 1 - closer approximation to the circle shape.

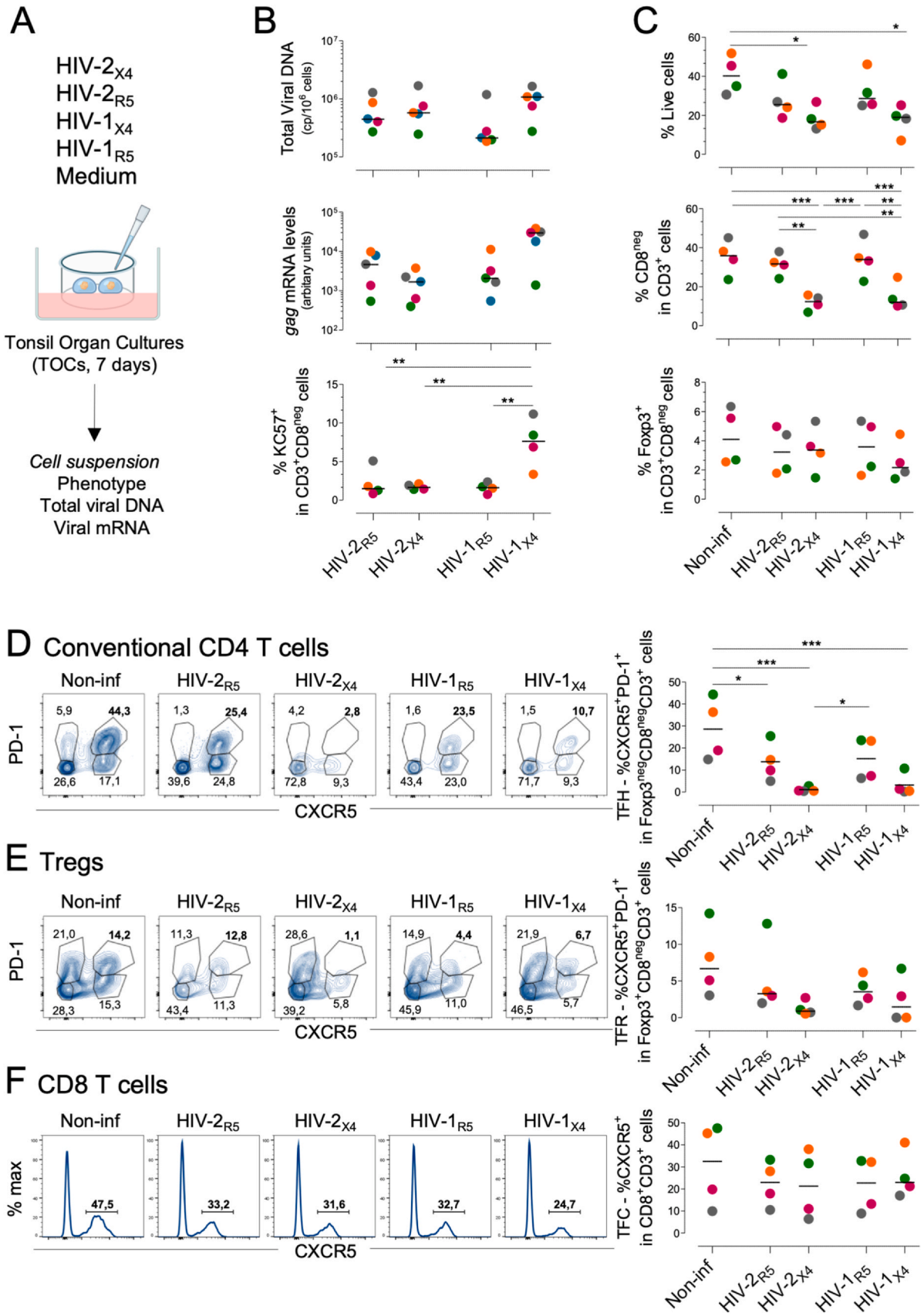

Fig. 3. HIV-2 infection of tonsil organ cultures (TOCs). (A) TOCs were infected with HIV-2 and HIV-1 primary isolates using the specified co-receptors; cell suspensions were generated at day 7 for RT-PCR and flow cytometry studies. (B) Viral parameters, namely: total cell-associated viral DNA (top); gag mRNA levels (centre); and frequency of KC57$^+$ (Gag$^+$) cells within CD4 T cells (bottom, defined as CD3$^+$CD8^{neg}). (C) Frequency of life cells (top), CD4$^+$ within T cells (centre, defined as CD3$^+$CD8^{neg}), and Foxp3$^+$ within CD4 T cells (bottom). (D-F) Representative plots and graphs showing the frequency of: (D) Follicular helper cells (TFH; CXCR5$^+$PD1$^+$) within conventional CD4 T cells (Foxp3^{neg}CD8^{neg}CD3$^+$); (E) Follicular regulatory cells (TFR; CXCR5$^+$PD1$^+$) within Tregs (Foxp3$^+$CD8^{neg}CD3$^+$); (F) Follicular cytotoxic cells (TFC; CXCR5+) within CD8 T cells (CD8$^+$CD3$^+$). Each dot colour in the graphs represents a different tonsil/subject. Bars represent the mean. p values < 0.05 after significant one-way ANOVA are shown namely: * < 0.05, ** < 0.01, and *** < 0.001.

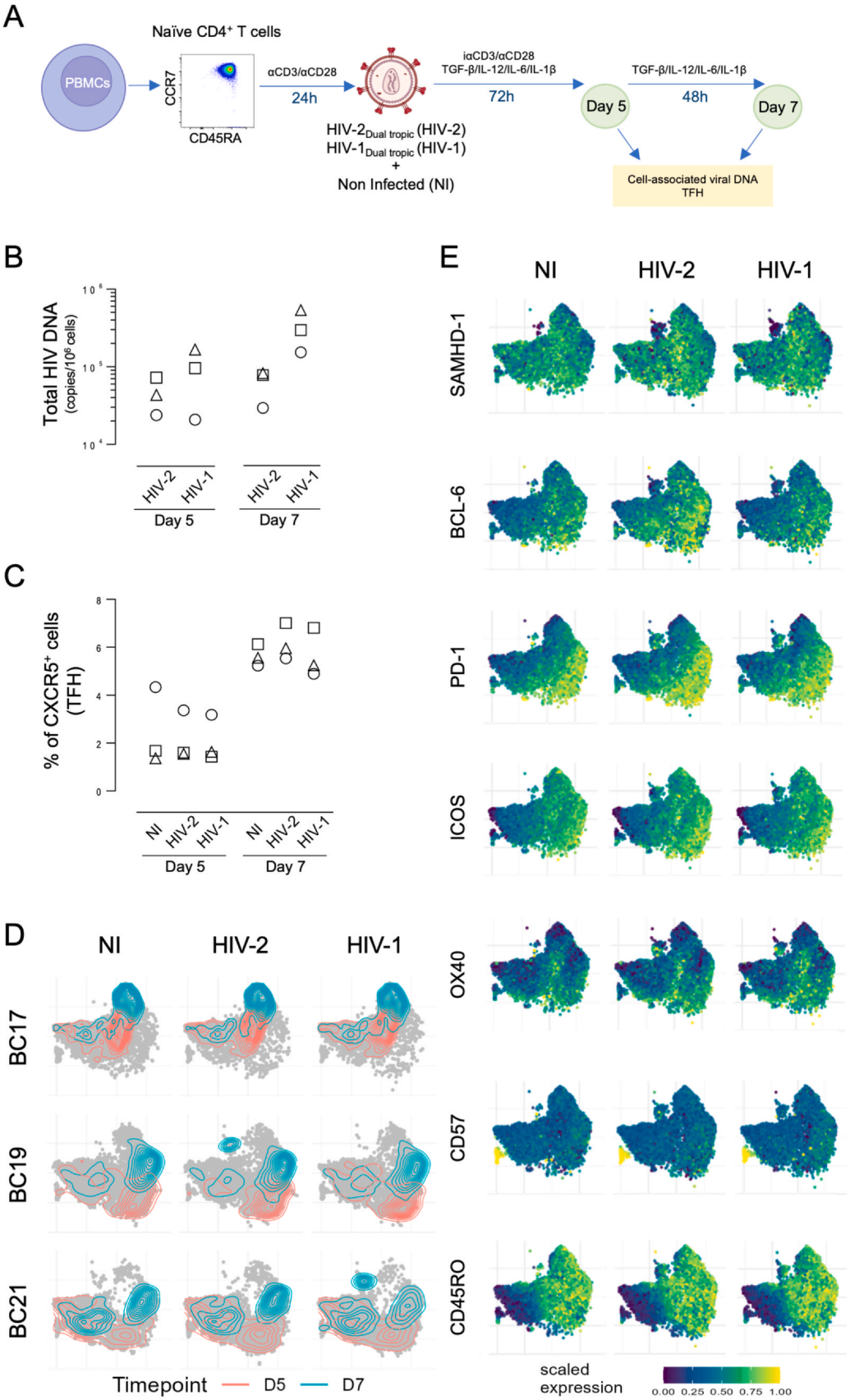

Fig. 4. TFH differentiation from naïve cells upon in vitro infection with HIV-2 or HIV-1. (A) Experimental design illustrating the naïve CD4 T cell isolation from peripheral blood, their infection by dual-tropic HIV-2 and HIV-1 primary isolates, and stimulation protocol for TFH differentiation. (B) Total cell-associated viral DNA at day 5 and 7 upon HIV-2 and HIV-1 infection of naïve CD4 T cells and culture in TFH differentiation conditions; each symbol represents a donor. (C) Frequency of CXCR5+ cells at day 5 and 7 in non-infected (NI) and infected by HIV-2 or HIV-1; each symbol represents a donor. (D) Comparison of the profile of cell differentiation at day 5 (red) and day 7 (blue), in the different donors and conditions; unsupervised analysis of flow cytometry data using UMAP. (E) Phenotypical analysis of TFH (CXCR5+) at day 7 using UMAP, concatenated data from the 3 donors in each condition are shown.

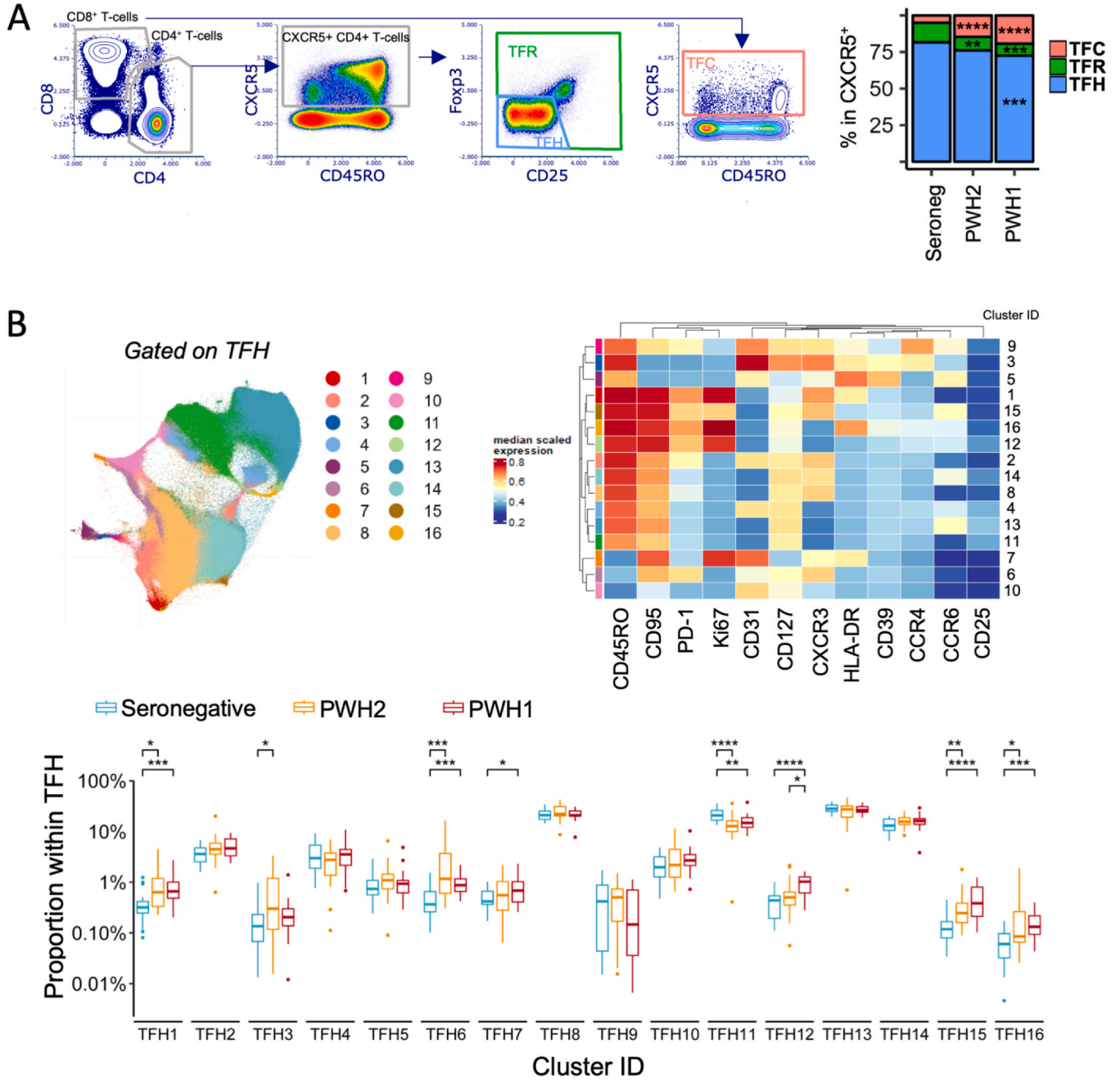

Fig. 5. Ex vivo analysis of circulating CXCR5+ T cells and phenotype of follicular helper T cells (TFH) in PWH2. (A) Illustrative manual analysis of the circulating follicular T cells to identify TFH, TFR and TFC; the stacked bar chart showing their mean proportion within total CXCR5+ cells in seronegative, PWH2 and PWH1. (B) Unsupervised analysis using UMAP of concatenated samples generated in spectral flow cytometry and gated on TFH cells (left), with colours representing the clusters defined in the heatmap (right). (C) Comparison of the distribution of the identified clusters within the 3 cohorts; boxplots represent median and interquartile range; *p* values < 0.05 after significant one-way ANOVA are shown, namely: * < 0.05, ** < 0.01, *** < 0.001, and **** < 0.0001.

and indirect signs, namely the perturbed phenotype of blood follicular lymphocytes and the impact of HIV-2 infection in organotypic in vitro cultures using tonsil tissue. These findings help uncover the mechanisms underlying the unique host-HIV-2 equilibrium,[4] characterised by a slow rate of disease progression without a significant impact on mortality,[12,14] and low-to-undetectable plasma viral load despite disseminated viral reservoirs[7–9] and persistent immune activation.[11,44,45]

We revealed significant ongoing viral replication in the lymph nodes using RNAscope, in agreement with a previous study examining 12 PWH2, which found a two-to-five-fold higher total proviral DNA in lymph node mononuclear cells than in PBMCs.[6] HIV-2 has been shown to have poor fitness and high cytopathogenicity in primary cells and tissues as compared to HIV-1 and SIV,[46,47] in line with the results provided here on HIV-2 infection of tonsil organ cultures. Moreover, the tonsil infection results confirmed our previous data generated using thymic infection assays,[33] supporting a post-transcriptional control of HIV-2 replication in primary cells without exogenous stimulation. Notably, the regulation of HIV-2 translation was shown to be distinct from HIV-1.[48,49] This distinct regulation likely impact on the efficiency of the viral production, and was associated with the accumulation HIV-2 RNA in stress granules in the absence of active translation.[49] The post-translational control may also be linked to the cell-intrinsic response induced by the HIV-

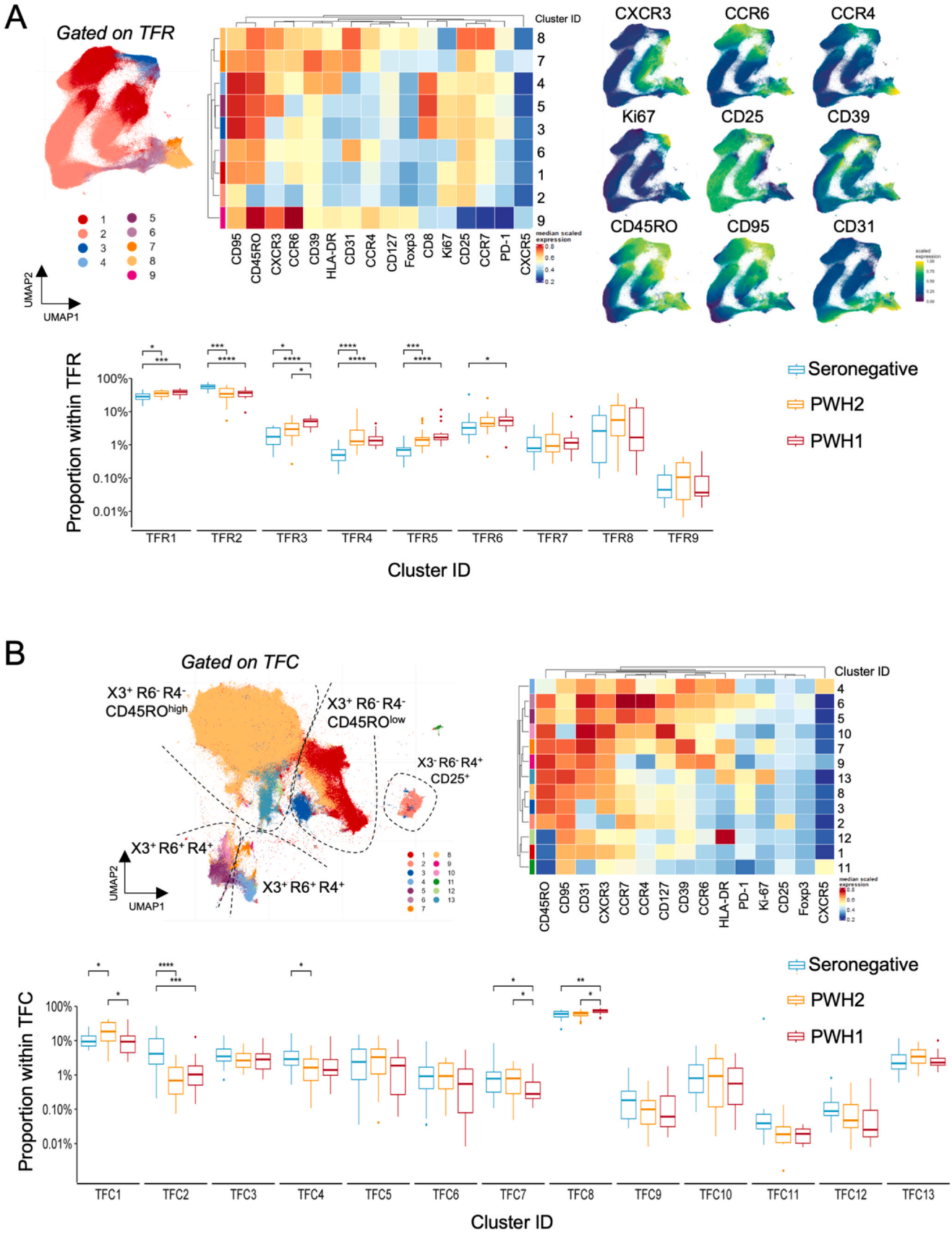

Fig. 6. Ex vivo analysis of circulating follicular regulatory T cells (TFR) and CXCR5+ CD8 T cells (TFC) in PWH2. (A) Unsupervised analysis using UMAP of concatenated samples generated in spectral flow cytometry and gated on TFR cells; expression of relevant markers is shown on the right; colours on the left UMAP plot represent the clusters defined in the heatmap; boxplots compare the distribution of the identified TFR clusters within the 3 cohorts. (B) Unsupervised analysis using UMAP of concatenated samples generated in spectral flow cytometry of gated TFC cells; colours represent the clusters defined in the heatmap, manually annotated based on the phenotype of the groups of clusters; boxplots compare the distribution of the identified TFC clusters within the 3 cohorts. Boxplots represent median and interquartile range; p values < 0.05 after significant one-way ANOVA are shown, namely: * < 0.05, ** < 0.01, *** < 0.001, and **** < 0.0001.

2 capside.[50] Interestingly, HIV-2 originated from multiple zoonotic transmissions of the SIVsm from sooty mangabeys to humans in West Africa,[4] but no significant impact on the lymph nodes was reported in the non-primate natural hosts of SIVsm despite the high viremia.[51] This finding further emphasise the relevance of HIV-2 infection to untangle the contribution of inflammatory components and cell-autonomous immunity to the pathology findings.[39,40,46,50,52–54]

The distinct cytopathogenicity[46,47] likely also impacts antigen presentation[50,53,54] and the sustainability of the specific responses.[15,16,19–21,26] In this study, we did not address in parallel the specific HIV-2 responses, known to be broad and sustained in PWH2.[15–22] Our work paves the way for future studies combining T and B cell receptor sequencing with new omics approaches[55–57] that are expected to spatially decipher the underlying mechanisms with implications for the development of therapeutic nAbs, engineered T cells and vaccines.[58,59] Additionally, these novel approaches may capture the transcriptomes of cells expressing viral mRNAs,[56,57,60] uncovering the biology of HIV-2-infected cells.

It is worth noting that we have previously shown that the gut mucosa integrity is preserved in PWH2, as well as the mucosal CD4 T cells, despite the presence of local active HIV-2 replication.[35] Thus, distinct tissue repair mechanisms are likely operating in secondary lymphoid organs and in the gut-associated lymphoid tissue in PWH2.

The prolonged infection also likely contributed to the disruption of the lymph node architecture and shaped the lymphocyte compartment in PWH2. Our results are in line with a previous study addressing the circulating follicular cell counterparts using a less extensive panel,[61] as well as with our previous data on the loss of memory B cells.[26,27] The significant imbalances found in the blood TFH phenotype warrant further functional validation, particularly regarding correlation with antibody titres, as has been done in PWH1 who were able to control the viremia, elite controllers,[62] and viremic.[63] We were unable to reveal a possible direct impact of the presence of HIV-2 on TFH differentiation, although these data should be interpreted with caution, given the limitations of the in vitro assays to address the differentiation of TFH from human naïve CD4 T cells.[34,64] The TFR imbalances were remarkably similar in PWH2 and PWH1, despite our finding of relatively better preserved Foxp3+ cells in the evaluated lymph nodes of PWH2 and the expected role of TFR in GC regulation.[41] We found a significant expansion of TFC and relative enrichment of cells with a stem-cell-like phenotype in PWH2, though our flow panel was not designed for cytotoxicity or stemness evaluation. Lymphoid tissue CD8 T cells have been emerging as determinants of pathology and HIV-1 control.[55,65–68] Thus, TFC arose as the key population to be further explored using spatial omics, in parallel with specificity and functional assays, to decipher the HIV-2-associated lymph node pathology.

Although our study was not designed to investigate the clinical features, immune phenotype and virological parameters of PWH2 under ART, the gathered results may help inform clinical decisions, given the paucity of data.[69]

Our investigations were constrained by sample size and the lack of longitudinal data due to the low prevalence of HIV-2 infection outside West Africa, where it is endemic.[31] We showed, nevertheless, using combined approaches that HIV-2 has a major impact on secondary lymphoid tissue organisation. The neglected HIV-2 infection represents an underexplored natural model to understand retroviral zoonoses and to identify strategies towards a functional HIV cure.

Funding

This work was funded by the following grants: PTDC/MED-IMU/30474/2017 to AES - project cofunded by FEDER LISBOA-01–0145-FEDER-030474, through POR Lisboa 2020 - Programa Operacional Regional de Lisboa, do PORTUGAL 2020 and Fundação para a Ciência e a Tecnologia (FCT); Gilead Genesis to SMF and AES; by national funding through FCT – Fundação para a Ciência e a Tecnologia, I.P., under the project PTDC/MED-IMU/0938/2020, DOI:10.54499/PTDC/MED-IMU/0938/2020 (Sousa, A.E., 2020). GBF received a fellowship funded by Janssen-Cilag Farmaceutica. AMCG received PhD scholarship from FCT (2020.10202. BD).

CRediT authorship contribution statement

Conceptualization: SMF, AGS, HNC, AES; Funding Acquisition: AES, SMF; Investigation: SMF, GBF, ARP, DFS, AVA, AP, RM, AGS, RTM, AMCG, HNC, PG, JP, CV, RB; Formal Analysis: SMF, GBF, ARP, DFS, AVA, AP, RM, AGS, CF, HNC; Data Curation: SMF, AGS, HNC, AES; Visualization: SMF, GBF, ARP, DFS, AVA, AP, RM, AES: Supervision: AES; Writing – Original Draft Preparation: SMF, AES; Writing – Review & Editing: all authors.

Declaration of Competing Interest

The authors declare that they have no known competing financial interests or personal relationships that could have appeared to influence the work reported in this paper.

Acknowledgements

We thank the clinicians Patricia Pacheco (Serviço de Infecciologia, Hospital Prof. Doutor Fernando da Fonseca, Unidade Local de Saúde Amadora/Sintra), Fernando Maltez (Doenças Infeciosas, Hospital Curry Cabral, Unidade Local de Saúde de São José), Rui M. M. Victorino and the ENT and Pathology departments of the Hospital de Santa Maria (ULSSM), the Instituto Português do Sangue e Transplantação (IPST) and all donors, patients, children, and their parents for their collaboration; Sandra Maurício, Cheila Rocha, Paula Matoso, Carolina Conceição, Amelia C. Trombetta, Bárbara Tavares, and Tiago Ferreira and Zoe I Junginger for experimental support; and the team members of Bioimaging, Histopathology, Flow Cytometry and Biosafety Level 3 facilities at GIMM – Gulbenkian Institute for Molecular Medicine (Lisbon, Portugal) for technical assistance.

Appendix A. Supplementary material

Supplementary data associated with this article can be found in the online version at doi:10.1016/j.jinf.2026.106760.

References

1. Pantaleo Giuseppe, Graziosi Cecilia, Demarest James F, Butini Luca, Montroni Maria, Fox Cecil H, et al. *HIV infection is active and progressive in lymphoid tissue during the clinically latent stage of disease. Nature* 1993;**362**(6418):355–8. https://doi.org/10.1038/362355a0
2. Banga Riddhima, Munoz Olivia, Perreau Matthieu. *HIV persistence in lymph nodes. Curr Opin HIV AIDS* 2021;**16**(4):209. https://doi.org/10.1097/COH.0000000000000686
3. Zeng Ming, Southern Peter J, Reilly Cavan S, Beilman Greg J, Chipman Jeffrey G, Schacker Timothy W, et al. *Lymphoid tissue damage in HIV-1 infection depletes naïve T cells and limits T cell reconstitution after antiretroviral therapy. PLoS Pathog* 2012;**8**(1):e1002437. https://doi.org/10.1371/journal.ppat.1002437
4. De Silva Thushan I, Cotten Matthew, Rowland-Jones Sarah L. *HIV-2: the forgotten AIDS virus. Trends Microbiol* 2008;**16**(12):588–95. https://doi.org/10.1016/j.tim.2008.09.003
5. Esbjörnsson Joakim, Jansson Marianne, Jespersen Sanne, Månsson Fredrik, Hønge BoL, Lindman Jacob, et al. *HIV-2 as a model to identify a functional HIV cure. AIDS Res Ther* 2019;**16**(1):24. https://doi.org/10.1186/s12981-019-0239-x
6. Jobe O, Ariyoshi K, Marchant A, Sabally S, Corrah T, Berry N, et al. *Proviral load and immune function in blood and lymph node during HIV-1 and HIV-2 infection. Clin Exp Immunol* 1999;**116**(3):474–8. https://doi.org/10.1046/j.1365-2249.1999.00914.x
7. Soares Rui S, Tendeiro Rita, Foxall Russell B, Baptista António P, Cavaleiro Rita, Gomes Perpétua, et al. *Cell-associated viral burden provides evidence of ongoing viral replication in aviremic HIV-2-Infected patients. J Virol* 2011;**85**(5):2429–38. https://doi.org/10.1128/JVI.01921-10

8. Bender Alexandra M, Simonetti Francesco R, Kumar Mithra R, Fray Emily J, Bruner Katherine M, Timmons Andrew E, et al. *The landscape of persistent viral genomes in ART-Treated SIV, SHIV, and HIV-2 Infections. Cell Host Microbe* 2019;**26**(1):73–85.e4. https://doi.org/10.1016/j.chom.2019.06.005
9. Koofhethile Catherine K, Gao Ce, Chang Charlotte, Lian Xiaodong, Shapiro Roger, Yu XuG, et al. *The HIV-2 proviral landscape is dominated by defective proviruses. AIDS* 2024;**38**(3):309–16. https://doi.org/10.1097/QAD.0000000000003776
10. Godinho-Santos Ana, Foxall Russell B, Antão Ana V, Tavares Bárbara, Ferreira Tiago, Serra-Caetano Ana, et al. *Follicular helper T cells are major human immunodeficiency Virus-2 reservoirs and support productive infection. J Infect Dis* 2020;**221**(1):122–6. https://doi.org/10.1093/infdis/jiz431
11. Sousa Ana E, Carneiro Jorge, Meier-Schellersheim Martin, Grossman Zvi, Victorino Rui MM. *CD4 T cell depletion is linked directly to immune activation in the pathogenesis of HIV-1 and HIV-2 but only indirectly to the viral load. J Immunol* 2002;**169**(6):3400–6. https://doi.org/10.4049/jimmunol.169.6.3400
12. Fryer Helen R, Van Tienen Carla, Van Der Loeff Maarten Schim, Aaby Peter, Da Silva Zacarias J, Whittle Hilton, et al. *Predicting the extinction of HIV-2 in rural Guinea-Bissau. AIDS* 2015;**29**(18):2479–86. https://doi.org/10.1097/QAD.0000000000000844
13. Esbjörnsson Joakim, Månsson Fredrik, Kvist Anders, Da Silva Zacarias J, Andersson Sören, Fenyö Eva Maria, et al. *Long-term follow-up of HIV-2-related AIDS and mortality in Guinea-Bissau: a prospective open cohort study. Lancet HIV* 2019;**6**(1):e25–31. https://doi.org/10.1016/S2352-3018(18)30254-6
14. Marlink Richard, Kanki Phyllis, Thior Ibou, Travers Karin, Eisen Geoffrey, Siby Tidiane, et al. *Reduced rate of disease development after HIV-2 infection as compared to HIV-1. Science* 1994;**265**(5178):1587–90. https://doi.org/10.1126/science.7915856
15. De Silva Thushan I, Aasa-Chapman Marlén, Cotten Matthew, Hué Stéphane, Robinson James, Bibollet-Ruche Frederic, et al. *Potent autologous and heterologous neutralizing antibody responses occur in HIV-2 infection across a broad range of infection outcomes. J Virol* 2012;**86**(2):930–46. https://doi.org/10.1128/JVI.06126-11
16. Karlsson Ingrid, Tingstedt Jeanette Linnea, Şahin Gülşen Özkaya, Hansen Mikkel, Szojka Zsofia, Buggert Marcus, et al. *Cross-reactive antibodies with the capacity to mediate hiv-1 envelope glycoprotein–targeted antibody-dependent cellular cytotoxicity identified in HIV-2–infected individuals. J Infect Dis* 2019;**219**(11):1749–54. https://doi.org/10.1093/infdis/jiz001
17. Kong Rui, Li Hui, Bibollet-Ruche Frederic, Decker Julie M, Zheng Natalie N, Gottlieb Geoffrey S, et al. *Broad and potent neutralizing antibody responses elicited in natural HIV-2 infection. J Virol* 2012;**86**(2):947–60. https://doi.org/10.1128/JVI.06155-11
18. Rodriguez Shaun K, Sarr Abdoulaye Dieng, MacNeil Adam, Thakore-Meloni Seema, Gueye-Ndiaye Aissatou, Traoré Ibrahima, et al. *Comparison of heterologous neutralizing antibody responses of human immunodeficiency virus type 1 (HIV-1)- and HIV-2-infected Senegalese patients: distinct patterns of breadth and magnitude distinguish HIV-1 and HIV-2 infections. J Virol* 2007;**81**(10):5331–8. https://doi.org/10.1128/JVI.02789-06
19. Foxall Russell B, Cortesão Catarina S, Albuquerque Adriana S, Soares Rui S, Victorino Rui MM, Sousa Ana E. *Gag-Specific CD4 $^{+}$ T-Cell frequency is inversely correlated with proviral load and directly correlated with immune activation in infection with human immunodeficiency virus Type 2 (HIV-2) but Not HIV-1. J Virol* 2008;**82**(19):9795–9. https://doi.org/10.1128/JVI.01217-08
20. Duvall Melody G, Jaye Assan, Dong Tao, Brenchley Jason M, Alabi Abraham S, Jeffries David J, et al. *Maintenance of HIV-Specific CD4+ T cell help distinguishes HIV-2 from HIV-1 Infection. J Immunol* 2006;**176**(11):6973–81. https://doi.org/10.4049/jimmunol.176.11.6973
21. Leligdowicz Aleksandra, Yindom Louis-Marie, Onyango Clayton, Sarge-Njie Ramu, Alabi Abraham, Cotten Matthew, et al. *Robust Gag-specific T cell responses characterize viremia control in HIV-2 infection. J Clin Invest* 2007;**117**(10):3067–74. https://doi.org/10.1172/JCI32380
22. De Silva Thushan I, Peng Yanchun, Leligdowicz Aleksandra, Zaidi Irfan, Li Lucy, Griffin Harry, et al. *Correlates of T-cell–mediated viral control and phenotype of CD8+ T cells in HIV-2, a naturally contained human retroviral infection. Blood* 2013;**121**(21):4330–9. https://doi.org/10.1182/blood-2012-12-472787
23. Esbjörnsson Joakim, Månsson Fredrik, Kvist Anders, Isberg Per-Erik, Nowroozalizadeh Salma, Biague Antonio J, et al. *Inhibition of HIV-1 disease progression by contemporaneous HIV-2 Infection. N Engl J Med* 2012;**367**(3):224–32. https://doi.org/10.1056/NEJMoa1113244
24. Rowland-Jones Sarah L, Whittle Hilton C. *Out of Africa: what can we learn from HIV-2 about protective immunity to HIV-1? Nat Immunol* 2007;**8**(4):329–31. https://doi.org/10.1038/ni0407-329
25. Marlink Richard. *Lessons from the second AIDS virus, HIV-2. AIDS* 1996;**10**:689–700. https://doi.org/10.1097/00002030-199606001-00002
26. Rocha Cheila, Duarte Joana, Borrego Pedro, Calado Rita, Marcelino José Maria, Tendeiro Rita, et al. *Potency of HIV-2-specific antibodies increase in direct association with loss of memory B cells. AIDS* 2017;**31**(17):2431–3. https://doi.org/10.1097/QAD.0000000000001661
27. Tendeiro Rita, Fernandes Sofia, Foxall Russell B, Marcelino José M, Taveira Nuno, Soares Rui S, et al. *Memory B-cell depletion is a feature of HIV-2 infection even in the absence of detectable viremia. AIDS* 2012;**26**(13):1607–17. https://doi.org/10.1097/QAD.0b013e3283568849
28. Pepin J, Dunn D, Gaye I, Alonso P, Egboga A, Tedder R, et al. *HIV-2 infection among prostitutes working in The Gambia: association with serological evidence of genital ulcer diseases and with generalized lymphadenopathy. AIDS* 1991;**5**(1):69–75.
29. Brun-Vezinet F, Katlama C, Roulot D, Lenoble L, Alizon M, Madjar JJ, et al. *LYMPHADENOPATHY-ASSOCIATED VIRUS TYPE 2 IN AIDS AND AIDS-RELATED COMPLEX: clinical and virological features in four patients. Lancet* 1987;**329**(8525):128–32. https://doi.org/10.1016/S0140-6736(87)91967-2
30. Clavel François, Mansinho Kamal, Chamaret Sophie, Guetard Denise, Favier Veronique, Nina Jaime, et al. *Human immunodeficiency virus Type 2 Infection associated with AIDS in West Africa. N Engl J Med* 1987;**316**(19):1180–5. https://doi.org/10.1056/NEJM198705073161903
31. Carvalho Ac, Valadas E, França L, Carvalho C, Aleixo Mj, Mendez J, et al. *Population mobility and the changing epidemics of HIV -2 in P ortugal. HIV Med* 2012;**13**(4):219–25. https://doi.org/10.1111/j.1468-1293.2011.00963.x
32. Pacheco Patrícia, Marques Nuno, Rodrigues Paulo, Mansinho Kamal, Maltez Fernando, Janeiro Nuno, et al. *Safety and efficacy of triple therapy with Dolutegravir Plus 2 nucleoside reverse transcriptase inhibitors in treatment-naive human immunodeficiency virus Type 2 patients: results from a 48-Week phase 2 study. Clin Infect Dis* 2023;**77**(5):740–8. https://doi.org/10.1093/cid/ciad339
33. Nunes-Cabaço Helena, Matoso Paula, Foxall Russell B, Tendeiro Rita, Pires Ana R, Carvalho Tânia, et al. *Thymic HIV-2 infection uncovers posttranscriptional control of viral replication in human thymocytes. J Virol* 2015;**89**(4):2201–8. https://doi.org/10.1128/JVI.03047-14
34. Schmitt Nathalie, Liu Yang, Bentebibel Salah-Eddine, Munagala Indira, Bourdery Laure, Venuprasad K, et al. *The cytokine TGF-β co-opts signaling via STAT3-STAT4 to promote the differentiation of human TFH cells. Nat Immunol* 2014;**15**(9):856–65. https://doi.org/10.1038/ni.2947
35. Fernandes SM, Pires AR, Matoso P, Ferreira C, Nunes-Cabaço H, Correia L, et al. *HIV-2 infection is associated with preserved GALT homeostasis and epithelial integrity despite ongoing mucosal viral replication. Mucosal Immunol* 2018;**11**(1):236–48. https://doi.org/10.1038/mi.2017.44
36. Glushakova Svetlana, Baibakov Boris, Margolis Leonid B, Zimmerberg Joshua. *Infection of human tonsil histocultures: a model for HIV pathogenesis. Nat Med* 1995;**1**(12):1320–2. https://doi.org/10.1038/nm1295-1320
37. Grivel Jean-Charles, Margolis Leonid. *Use of human tissue explants to study human infectious agents. Nat Protoc* 2009;**4**(2):256–69. https://doi.org/10.1038/nprot.2008.245
38. Cai Yanhui, Abdel-Mohsen Mohamed, Tomescu Costin, Xue Fengtian, Wu Guoxin, Howell Bonnie J, et al. *BCL6 Inhibitor-mediated downregulation of phosphorylated SAMHD1 and T cell activation are associated with decreased HIV infection and reactivation. J Virol* 2019;**93**(2):e01073-18. https://doi.org/10.1128/JVI.01073-18
39. Baldauf Hanna-Mari, Pan Xiaoyu, Erikson Elina, Schmidt Sarah, Daddacha Waaqo, Burggraf Manja, et al. *SAMHD1 restricts HIV-1 infection in resting CD4+ T cells. Nat Med* 2012;**18**(11):1682–8. https://doi.org/10.1038/nm.2964
40. Baldauf Hanna-Mari, Stegmann Lena, Schwarz Sarah-Marie, Ambiel Ina, Trotard Maud, Martin Margarethe, et al. *Vpx overcomes a SAMHD1-independent block to HIV reverse transcription that is specific to resting CD4 T cells. Proc Natl Acad Sci USA* 2017;**114**(10):2729–34. https://doi.org/10.1073/pnas.1613635114
41. Fonseca Valter R, Agua-Doce Ana, Maceiras Ana Raquel, Pierson Wim, Ribeiro Filipa, Romão Vasco C, et al. *Human blood Tfr cells are indicators of ongoing humoral activity not fully licensed with suppressive function. Sci Immunol* 2017;**2**(14):eaan1487. https://doi.org/10.1126/sciimmunol.aan1487
42. Bird Prudence, Lachmann Peter J. *The regulation of IgG subclass production in man: low serum IgG4 in inherited deficiencies of the classical pathway of C3 activation. Eur J Immunol* 1988;**18**(8):1217–22. https://doi.org/10.1002/eji.1830180811
43. Blanco Elena, Pérez-Andrés Martín, Arriba-Méndez Sonia, Serrano Cristina, Criado Ignacio, Del Pino-Molina Lucía, et al. *Defects in memory B-cell and plasma cell subsets expressing different immunoglobulin-subclasses in patients with CVID and immunoglobulin subclass deficiencies. J Allergy Clin Immunol* 2019;**144**(3):809–24. https://doi.org/10.1016/j.jaci.2019.02.017
44. Grossman Zvi, Meier-Schellersheim Martin, Sousa Ana E, Victorino Rui MM, Paul William E. *CD4+ T-cell depletion in HIV infection: are we closer to understanding the cause? Nat Med* 2002;**8**(4):319–23. https://doi.org/10.1038/nm0402-319
45. Johansson Emil, Nazziwa Jamirah, Freyhult Eva, Hong Mun-Gwan, Lindman Jacob, Neptin Malin, et al. *HIV-2 MEDIATED EFFECTS ON TARGET AND BYSTANDER CELLS INDUCE PLASMA PROTEOME REMODELLING. iScience* 2024;**27**:109344. https://doi.org/10.1016/j.isci.2024.109344
46. Tebit Denis M, Nickel Gabrielle, Gibson Richard, Rodriguez Myriam, Hathaway Nicolas J, Bain Katie, et al. *Replicative fitness and pathogenicity of primate lentiviruses in lymphoid tissue, primary human and chimpanzee cells: relation to possible jumps to humans. eBioMedicine* 2024;**100**:104965. https://doi.org/10.1016/j.ebiom.2023.104965
47. Schramm B, Penn ML, Palacios EH, Grant RM, Kirchhoff F, Goldsmith MA. *Cytopathicity of human immunodeficiency virus type 2 (HIV-2) in human lymphoid tissue is coreceptor dependent and comparable to that of HIV-1. J Virol* 2000;**74**(20):9594–600. https://doi.org/10.1128/jvi.74.20.9594-9600.2000
48. Soto-Rifo R, Limousin T, Rubilar PS, Ricci EP, Decimo D, Moncorge O, et al. *Different effects of the TAR structure on HIV-1 and HIV-2 genomic RNA translation. Nucleic Acids Res* 2012;**40**(6):2653–67. https://doi.org/10.1093/nar/gkr1093
49. Soto-Rifo Ricardo, Valiente-Echeverria Fernando, Rubilar Paulina S, Garcia-de-Gracia Francisco, Ricci Emiliano P, Limousin Taran, et al. *HIV-2 genomic RNA accumulates in stress granules in the absence of active translation. Nucleic Acids Res* 2014;**42**(20):12861–75. https://doi.org/10.1093/nar/gku1017
50. Lahaye Xavier, Gentili Matteo, Silvin Aymeric, Conrad Cécile, Picard Léa, Jouve Mabel, et al. *NONO detects the nuclear HIV capsid to promote cGAS-mediated innate immune activation. Cell* 2018;**175**(2):488–501.e22. https://doi.org/10.1016/j.cell.2018.08.062
51. Silvestri Guido, Sodora Donald L, Koup Richard A, Paiardini Mirko, O'Neil Shawn P, McClure Harold M, et al. *Nonpathogenic SIV infection of sooty mangabeys is characterized by limited bystander immunopathology despite chronic high-level Viremia. Immunity* 2003;**18**(3):441–52. https://doi.org/10.1016/S1074-7613(03)00060-8
52. Zhang Kunli, Huang Qiuyan, Li Xinming, Zhao Ziqiao, Hong Chun, Sun Zeyi, et al. *The cGAS-STING pathway in viral infections: a promising link between inflammation,*

oxidative stress and autophagy. Front Immunol 2024;**15**:1352479. https://doi.org/10.3389/fimmu.2024.1352479
53. Lahaye Xavier, Satoh Takeshi, Gentili Matteo, Cerboni Silvia, Conrad Cécile, Hurbain Ilse, et al. *The capsids of HIV-1 and HIV-2 determine immune detection of the viral cDNA by the innate sensor cGAS in dendritic cells. Immunity* 2013;**39**(6):1132–42. https://doi.org/10.1016/j.immuni.2013.11.002
54. Cabral-Piccin Mariela P, Papagno Laura, Lahaye Xavier, Perdomo-Celis Federico, Volant Stevenn, White Eoghann, et al. *Primary role of type I interferons for the induction of functionally optimal antigen-specific CD8+ T cells in HIV infection. eBioMedicine* 2023;**91**:104557. https://doi.org/10.1016/j.ebiom.2023.104557
55. Papadopoulos Andrea O, Mvaya Leonard, Khaba Trevor, Ngema Namani, Smidt Werner, Msipa Sibongiseni, et al. *Spatial regulation of CD8+ T cells at the HLA-E-NKG2A axis drives HIV persistence in lymph node B cell follicles. Cell Rep* 2025;**44**(9):116181. https://doi.org/10.1016/j.celrep.2025.116181
56. Hu Kevin, O'Neil Thomas R, Baharlou Heeva, Austin Paul J, Karrasch Jackson F, Sarkawt Lara, et al. *The spatial biology of HIV infection. PLOS Pathog* 2025;**21**(1):e1012888. https://doi.org/10.1371/journal.ppat.1012888
57. Zaman Fatima, Smith Melissa L, Balagopal Ashwin, Durand Christine M, Redd Andrew D, Tobian Aaron AR. *Spatial technologies to evaluate the HIV-1 reservoir and its microenvironment in the lymph node. mBio* 2024;**15**(8):e01909-24. https://doi.org/10.1128/mbio.01909-24
58. Haynes Barton F, Wiehe Kevin, Borrow Persephone, Saunders Kevin O, Korber Bette, Wagh Kshitij, et al. *Strategies for HIV-1 vaccines that induce broadly neutralizing antibodies. Nat Rev Immunol* 2023;**23**(3):142–58. https://doi.org/10.1038/s41577-022-00753-w
59. Havenar-Daughton Colin, Lee Jeong Hyun, Crotty Shane. *Tfh cells and HIV bnAbs, an immunodominance model of the HIV neutralizing antibody generation problem. Immunol Rev* 2017;**275**(1):49–61. https://doi.org/10.1111/imr.12512
60. Plasek Hegde Leah M, Gunawardane Lalith S, Niazi Farshad, Mbonye Uri, Leskov Konstantin, Perez Gani, et al. *HIV infection reprogrammes CD4+ T cells for quiescence and entry into proviral latency. Nat Microbiol* 2025;**10**(10):2454–71. https://doi.org/10.1038/s41564-025-02128-y
61. Ponnan Sivasankaran Munusamy, Vidyavijayan KK, Thiruvengadam Kannan, Hilda J Nancy, Mathayan Manikannan, Murugavel Kailapuri Gangatharan, et al. *Role of circulating T follicular helper cells and stem-like memory CD4+ T cells in the pathogenesis of HIV-2 infection and disease progression. Front Immunol* 2021;**12**:666388. https://doi.org/10.3389/fimmu.2021.666388
62. Martin-Gayo Enrique, Cronin Jacqueline, Hickman Taylor, Ouyang Zhengyu, Lindqvist Madelene, Kolb Kellie E, et al. *Circulating CXCR5$^+$CXCR3$^+$PD-1^{lo} Tfh-like cells in HIV-1 controllers with neutralizing antibody breadth. JCI Insight* 2017;**2**(2):e89574. https://doi.org/10.1172/jci.insight.89574
63. Noto Alessandra, Suffiotti Madeleine, Joo Victor, Mancarella Antonio, Procopio Francesco A, Cavet Guy, et al. *The deficiency in Th2-like Tfh cells affects the maturation and quality of HIV-specific B cell response in viremic infection. Front Immunol* 2022;**13**:960120. https://doi.org/10.3389/fimmu.2022.960120
64. Locci Michela, Wu Jennifer E, Arumemi Fortuna, Mikulski Zbigniew, Dahlberg Carol, Miller Andrew T, et al. *Activin a programs the differentiation of human TFH cells. Nat Immunol* 2016;**17**(8):976–84. https://doi.org/10.1038/ni.3494
65. Petrovas Constantinos, Ferrando-Martinez Sara, Gerner Michael Y, Casazza Joseph P, Pegu Amarendra, Deleage Claire, et al. *Follicular CD8 T cells accumulate in HIV infection and can kill infected cells in vitro via bispecific antibodies. Sci Transl Med* 2017;**9**(373):eaag2285. https://doi.org/10.1126/scitranslmed.aag2285
66. He Ran, Hou Shiyue, Liu Cheng, Zhang Anli, Bai Qiang, Han Miao, et al. *Follicular CXCR5-expressing CD8+ T cells curtail chronic viral infection. Nature* 2016;**537**(7620):412–6. https://doi.org/10.1038/nature19317
67. Nguyen Son, Deleage Claire, Darko Samuel, Ransier Amy, Truong Duc P, Agarwal Divyansh, et al. *Elite control of HIV is associated with distinct functional and transcriptional signatures in lymphoid tissue CD8+ T cells. Sci Transl Med* 2019;**11**(523):eaax4077. https://doi.org/10.1126/scitranslmed.aax4077
68. Rutishauser Rachel L, Deguit Christian Deo T, Hiatt Joseph, Blaeschke Franziska, Roth Theodore L, Wang Lynn, et al. *TCF-1 regulates HIV-specific CD8$^+$ T cell expansion capacity. JCI Insight* 2021;**6**(3):e136648. https://doi.org/10.1172/jci.insight.136648
69. Gottlieb Geoffrey S, Raugi Dana N, Smith Robert A. *90-90-90 for HIV-2? Ending the HIV-2 epidemic by enhancing care and clinical management of patients infected with HIV-2. Lancet HIV* 2018;**5**(7):e390–9. https://doi.org/10.1016/S2352-3018(18)30094-8